

## REPORT 1256

### AXIALLY SYMMETRIC SHAPES WITH MINIMUM WAVE DRAG<sup>1</sup>

By MAX. A. HEASLET and FRANKLYN B. FULLER

#### SUMMARY

*The external wave drag of bodies of revolution moving at supersonic speeds can be expressed either in terms of the geometry of the body, or in terms of the body-simulating axial source distribution. For purposes of deriving optimum bodies under various given conditions, it is found that the second of the methods mentioned is the more tractable. By use of a quasi-cylindrical theory, that is, the boundary conditions are applied on the surface of a cylinder rather than on the body itself, the variational problems of the optimum bodies having prescribed volume or caliber are solved. The streamwise variations of cross-sectional area and drags of the bodies are exhibited, and some numerical results are given. The solutions are found to depend upon a single parameter involving Mach number and the radius-length ratio of the given cylinder. Variation of this parameter from zero to infinity gives the spectrum of optimum bodies, for the prescribed condition, from the slender-body result to the two-dimensional. The numerical results show that for increasing values of the parameter, the optimum shapes quickly approach the two-dimensional.*

*A reciprocity relation for axial flow is derived, and it is used in formulating the variational problems in terms of the drag formula involving geometry. Formulation of the minimum problems in terms of combined flow fields is found to lead to extremely simple relations that are satisfied by the flow field induced by optimum bodies. The combined flow concepts are also useful, for example, in checking results found by other means.*

#### INTRODUCTION

The design of minimum-drag configurations is one of the fundamental problems of aerodynamics. For many engineering purposes it is, furthermore, possible to make useful predictions and design calculations for steady flight by considering additively the drag attributable to the viscous nature of the air and the drag that occurs in an inviscid medium. Since efficient flight is closely associated with the use of aerodynamic shapes producing relatively small disturbances in the air, the analysis upon which the inviscid-fluid theory is based can, in many cases of practical interest, be further limited to first-order approximations involving small perturbations. For supersonic flight speeds such an analysis is linear, the perturbation velocity potential of the flow field satisfies the wave equation, and the pressure drag of nonlifting configurations results from the accumulation of energy in the waves induced by the body during its motion.

The purpose of the present paper is to show how most

favorable body shapes, under various given conditions, can be derived by using formulae for drag prediction that are based upon the linearized theory. The type of body to be treated is a nacelle- or duct-like configuration (nonlifting and having axial symmetry) which induces perturbations that are specified on the surface of a circular cylinder. The analysis might be termed quasi-cylindrical, since boundary conditions are applied on the surface of a cylinder rather than on the body itself. Only the external flow is considered.

There are two rather different methods available for the calculation of drag of such bodies. The first, given by Ward in reference 1, expresses the drag in terms of the geometry of the body and of a weighting function first encountered by Lighthill (ref. 2) in connection with the drag of fusiform bodies. The second result, published recently by Parker (ref. 3), is a formula in which the drag is expressed in terms of the strength of an axial source distribution that simulates the body shape. Generally speaking, the formula giving drag directly in terms of geometrical characteristics would be preferable, since the usual auxiliary conditions in variation problems, such as given volume, given caliber, etc., are also expressed in geometrical terms. Unfortunately, however, the variational problem in this case leads to an integral equation whose kernel is the Lighthill function mentioned previously, and the properties of this function are not at present well enough known to enable one to solve the integral equation by other than numerical methods. On the other hand, the expression for drag in terms of sources leads to a tractable integral equation, although the relations between source strength and geometry are somewhat complex.

Problems of the sort to be treated here have been attacked by Ferrari (refs. 4 and 5) and by Parker (ref. 3). The first-named author has approached the problem of minimum drag with assorted isoperimetric conditions by both the above-mentioned methods, but the main effort was made in connection with the source-strength method applied in conjunction with a control surface consisting of a frustum of a cone. A large number of cases have been worked out, mostly by numerical methods. The other work, reference 3, gives a solution to the problem of the minimum-drag body with given caliber, making use of boundary conditions on the Stokes' stream function, rather than the potential function.

In this paper we shall approach the problem by the use of both methods outlined above. In an introductory section, the operational approach to the wave equation is extended to bodies having peripheral as well as longitudinal variations

<sup>1</sup>Supersedes NACA TN 3389 by Max. A. Heaslet and Franklyn B. Fuller, 1955.

of surface shape. The analysis is then restricted to the case of axial symmetry and the two drag formulae are given. Then a reciprocity relation for axial flow is derived, and the notion of combined flow fields is introduced. This device leads, through application of the reciprocity relation and the drag formula in terms of body geometry, to extremely simple physical characterizations of the flow fields associated with optimum bodies. Next, in order to derive explicit expressions for some optimum bodies we consider the source-function approach in combination with a cylindrical control surface on which boundary conditions are specified. The results obtained are discussed with the aid of numerical examples, and, finally, the reciprocity relations derived earlier are exhibited in terms of the explicit solutions found, and some uses of the reciprocity results are indicated.

The appendix is devoted to summarizing the results of the minimizations for the convenience of the reader.

**LIST OF IMPORTANT SYMBOLS**

|                 |  |
|-----------------|--|
| $a_0$           | speed of sound in free stream  |
| $A_0(x)$        | strength of source distribution  |
| $B(\sigma)$     | function used in isoperimetric problems (See eqs. (60).)                           |
| $C_p$           | pressure coefficient, $\frac{p-p_0}{q_0}$  |
| $D$             | drag   |
| $E$             | complete elliptic integral of second kind of modulus $k$                           |
| $k$             | modulus of elliptic integrals  |
| $K$             | complete elliptic integral of first kind of modulus $k$                            |
| $K_m, I_m$      | Bessel functions of order $m$ (See ref. 8.)  |
| $l$             | length of body   |
| $M_0$           | Mach number in the free stream, $\frac{U_0}{a_0}$                                  |
| $n_1, n_2, n_3$ | direction cosines with respect to Cartesian axes of the inward normal to a surface |
| $p$             | pressure   |
| $p_0$           | pressure in the free stream  |
| $P$             | pressure in a combined flow field, $p - \tilde{p}$                                 |
| $q_0$           | dynamic pressure, $\frac{1}{2} \rho_0 U_0^2$                                       |
| $r$             | radial coordinate, $\sqrt{y^2 + z^2}$  |
| $\Delta r(x)$   | incremental radius on control cylinder due to source distribution along axis       |
| $R$             | radius of cylindrical control surface  |
| $S(x)$          | cross-sectional area of a body   |
| $\Delta S(x)$   | $S(x) - S(0)$  |
| $x, y, z$       | Cartesian coordinates  |
| $u, v, w$       | perturbation velocities in $x, y, z$ directions, respectively                      |
| $U_0$           | free-stream velocity   |
| $v_r$           | perturbation velocity in radial direction  |
| $V$             | volume of body   |
| $V_0$           | additional volume wrapped on cylindrical control surface.                          |
| $W(z)$          | function defined in equation (25)  |
| $\alpha^2$      | parameter of elliptic integral of third kind                                       |
| $\beta^2$       | $M_0^2 - 1$  |
| $\eta$          | dimensionless streamwise coordinate, $\frac{x}{l}$                                 |

|                    |   |
|--------------------|---|
| $\theta$           | angular coordinate, $\tan^{-1} \frac{z}{y}$   |
| $\lambda, \mu$     | Lagrange multipliers in isoperimetric problems  |
| $\Pi(\alpha^2, k)$ | complete elliptic integral of third kind of modulus $k$ and parameter $\alpha^2$ (in notation of ref. 20) |
| $\rho_0$           | free-stream density   |
| $\sigma$           | $\frac{\beta R}{l}$   |
| $\varphi$          | perturbation velocity potential   |

**SUFFIXES**

|   |  |
|---|--|
| ' | differentiation with respect to streamwise coordinate                          |
| ~ | quantity evaluated in reversed flow field                                      |
| - | Laplace transform  |
| * | dimensionless quantity as $V^* = \frac{V}{l^2}$ , $S^* = \frac{S}{l^2}$ , etc. |

**INTRODUCTORY ANALYSIS**

The analysis to be given here is adapted to boundary conditions specified on a right circular cylinder so oriented that its axis is parallel to the free-stream velocity vector. Immediate application thus follows for quasi-cylindrical shapes that deviate slightly, both longitudinally and peripherally, from a cylindrical control surface although the expression for drag can be extended to include the domain of slender-body theory.

Consider a fixed Cartesian coordinate system in a supersonic free-stream of velocity  $U_0$  and Mach number  $M_0 = U_0/a_0 > 1$  where  $a_0$  is the velocity of sound in the free stream. The  $x$  axis is aligned with the direction of the flow and the lateral coordinates  $y, z$  may also be expressed in polar coordinates  $r, \theta$  where  $r = \sqrt{y^2 + z^2}$ ,  $\theta = \tan^{-1} z/y$ . A cylindrical control surface of radius  $r = R = \text{const.}$  is given with the range  $0 \leq x \leq l$  and on this control surface the perturbation velocity components, together with their gradients, are small relative to  $U_0$  and  $U_0/l$ . Under these conditions the field external to the cylinder of radius  $R$  has for its governing equation the linear relation

$$\beta^2 \varphi_{xx} - \varphi_{yy} - \varphi_{zz} = 0 \tag{1}$$

where the subscript notation denotes partial differentiation,  $\varphi(x, y, z)$  is the perturbation velocity potential yielding the perturbation velocity components

$$u(x, y, z) = \varphi_x(x, y, z), \quad v(x, y, z) = \varphi_y(x, y, z), \quad w(x, y, z) = \varphi_z(x, y, z)$$

and  $\beta^2 = M_0^2 - 1$ . The boundary conditions on the body are to be taken in the form

$$\varphi_r(x, r, \theta)|_{r=R} = U_0 G(x, \theta), \quad 0 \leq x \leq l \tag{2}$$

where  $G$  is a known function of  $x$  and  $\theta$ .

**A GENERAL SOLUTION OF THE WAVE EQUATION IN CYLINDRICAL COORDINATES**

If equation (1) is rewritten in the form

$$\beta^2 \varphi_{xx} - \varphi_{rr} - (1/r) \varphi_r - (1/r)^2 \varphi_{\theta\theta} = 0 \tag{3}$$

it is possible, through separation of variables, to derive a general solution representing a rectilinear distribution of

source and multipole singularities. This general solution can be found by use of the Laplace transformation. By definition, the Laplace transform<sup>2</sup> (see ref. 6) of a function  $F(x, r, \theta)$  is  $\bar{F}(s; r, \theta)$  where

$$\bar{F}(s; r, \theta) = \int_0^\infty e^{-sx} F(x, r, \theta) dx \quad (4)$$

If one employs this transformation and applies initial conditions consistent with supersonic flow theory (ref. 7), equation (3) becomes

$$\beta^2 s^2 \bar{\varphi} - \bar{\varphi}_{rr} - (1/r) \bar{\varphi}_r - (1/r)^2 \bar{\varphi}_{\theta\theta} = 0 \quad (5)$$

The transform of the perturbation velocity potential is assumed separable in the form

$$\bar{\varphi}(s; r, \theta) = \zeta(r, s) \cos m\theta$$

and it follows directly that  $\zeta(r, s)$  must satisfy the ordinary differential equation

$$\frac{d^2 \zeta}{d(\beta r s)^2} + \frac{1}{\beta r s} \frac{d\zeta}{d(\beta r s)} - \left[ 1 + \frac{m^2}{(\beta r s)^2} \right] \zeta = 0$$

Thus, the solution can be written

$$\bar{\varphi}(s; r, \theta) = -\frac{1}{2\pi} \sum_0^\infty \cos m\theta [\bar{A}_m(s) K_m(\beta r s) + \bar{B}_m(s) I_m(\beta r s)]$$

where  $K_m$  and  $I_m$  are modified Bessel functions in the notation of reference 8. The asymptotic expansions for the Bessel functions show that  $I_m$  yields incoming waves suitable for the analysis of flow inside a tube or cylindrical control surface;  $K_m$  yields outgoing waves that are suited to the calculation of the field external to a tube. It follows that one has, in the latter case,

$$\bar{\varphi}(s; r, \theta) = -\frac{1}{2\pi} \sum_0^\infty \bar{A}_m(s) K_m(\beta r s) \cos m\theta \quad (6)$$

The inversion of equation (6) can be achieved in two ways. First, from reference 9, page 277, and the convolution integral, one gets

$$\varphi(x, r, \theta) = -\frac{1}{2\pi} \left[ \int_0^{x-\beta r} \frac{A_0(x_1) dx_1}{\sqrt{(x-x_1)^2 - \beta^2 r^2}} + \sum_1^\infty \cos m\theta \int_0^{x-\beta r} \frac{A_m(x_1) \cosh \left( m \cosh^{-1} \frac{x-x_1}{\beta r} \right) dx_1}{\sqrt{(x-x_1)^2 - \beta^2 r^2}} \right] \quad (7)$$

Second (see, e. g., ref. 8, p. 79), one has

$$K_m(\beta r s) = (-1)^m \frac{r^m}{\beta^m s^m} \left( \frac{d}{dr} \right)^m K_0(\beta r s)$$

Thus equation (6) can be rewritten as

$$\bar{\varphi}(s; r, \theta) = -\frac{1}{2\pi} \left[ A_0(s) K_0(\beta r s) + \sum_1^\infty \left( -\frac{r}{\beta} \right)^m \cos m\theta \left( \frac{d}{dr} \right)^m \frac{\bar{A}_m(s)}{s^m} K_0(\beta r s) \right]$$

and the inversion is

$$\varphi(x, r, \theta) = -\frac{1}{2\pi} \left[ \int_0^{x-\beta r} \frac{A_0(x_1) dx_1}{\sqrt{(x-x_1)^2 - \beta^2 r^2}} + \sum_1^\infty \left( -\frac{r}{\beta} \right)^m \cos m\theta \left( \frac{d}{dr} \right)^m \int_0^{x-\beta r} \frac{C_m(x_1) dx_1}{\sqrt{(x-x_1)^2 - \beta^2 r^2}} \right] \quad (8)$$

where the function  $C_m(x)$  is given by (from operational calculus rules)

$$\begin{aligned} C_m(x) &= \int_0^x dx_m \cdot \dots \cdot \int_0^{x_2} dx_2 \int_0^{x_2} A_m(x_1) dx_1 \\ &= \frac{1}{(m-1)!} \int_0^x (x-x_1)^{m-1} A_m(x_1) dx_1 \end{aligned} \quad (9)$$

Equation (8) expresses the solution in the usual form, given, for example, in reference 10, page 527. For some purposes, numerical calculations for example, equation (7) has advantages over equation (8). The two solutions express the perturbation velocity potential in terms of distributions of singularities along the central axis, the first term representing a distribution of supersonic sources of strength  $A_0(x) dx$ , and the subsequent terms representing multipoles of order  $m$ .

It is of interest to calculate the limiting forms of equations (7) and (8) for large and small values of  $r$ . For large  $r$ , equation (6) becomes

$$\bar{\varphi}(s; r, \theta) \sim -\frac{1}{2\pi} \sum_0^\infty \bar{A}_m(s) \sqrt{\frac{\pi}{2\beta r s}} e^{-\beta r s} \cos m\theta \quad (10)$$

where the asymptotic form

$$K_m(z) \sim \sqrt{\frac{\pi}{2z}} e^{-z}$$

has been used. The perturbation velocity potential is then

$$\varphi(x, r, \theta) \sim -\frac{1}{2\pi \sqrt{2\beta r}} \sum_0^\infty \cos m\theta \int_0^{x-\beta r} A_m(\xi) \frac{d\xi}{\sqrt{x-\xi-\beta r}} \quad (11)$$

The ultimate attenuation of  $\varphi$  with lateral distance is therefore fixed by the factor  $1/\sqrt{r}$ . For small  $r$ , equation (6) becomes

$$\begin{aligned} \bar{\varphi}(s; r, \theta) &\approx -\frac{1}{2\pi} \left[ -\bar{A}_0(s) \left( \ln \frac{\beta r s}{2} + \gamma \right) + \sum_1^\infty \frac{\bar{A}_m(s)}{2} (m-1)! \left( \frac{2}{\beta r s} \right)^m \cos m\theta \right] \end{aligned} \quad (12)$$

where  $\gamma = 0.577$  is Euler's constant. The inversion of equation (12) is

$$\begin{aligned} \varphi(x, r, \theta) &\approx \frac{1}{2\pi} \left[ A_0(x) \ln \frac{\beta r}{2} + \frac{\partial}{\partial x} \int_0^x A_0(x_1) \ln |x-x_1| dx_1 + \sum_1^\infty \left( \frac{2}{\beta r} \right)^m \frac{(m-1)!}{2} \cos m\theta C_m(x) \right] \end{aligned} \quad (13)$$

where  $C_m(x)$  is defined in equation (9). This result was used by Ward (ref. 11) as a basis for the development of slender-body theory.

<sup>2</sup> It will be assumed through the present section that the origin lies upstream of all disturbance points in the flow field. Subsequently, the origin will be shifted so as to lie at the upstream face of the control surface or body.

As presented, the above general solutions (eqs. (7) and (8)) were not related to specific boundary conditions. The formal development of this relation is straightforward and leads to an explicit solution for boundary conditions given on the cylindrical control surface at  $r=R=\text{const}$ . Let the given conditions be

$$\varphi_r|_{r=R} = U_o G(x, \theta) = U_o \sum_0^{\infty} g_m(x) \cos m\theta \quad (14)$$

From equations (6) and (14), one has

$$\begin{aligned} \bar{\varphi}_r(s; r, \theta)|_{r=R} &= -\frac{1}{2\pi} \sum_0^{\infty} \bar{A}_m(s) \left[ \frac{d}{dr} K_m(\beta r s) \right]_{r=R} \cos m\theta \\ &= U_o \sum_0^{\infty} \bar{g}_m(s) \cos m\theta \end{aligned} \quad (15)$$

Since

$$\frac{d}{dr} K_m(\beta r s) = \beta s K_m'(\beta r s)$$

equation (15) yields

$$\bar{A}_m(s) = -\frac{2\pi U_o}{\beta} \frac{\bar{g}_m(s)}{s K_m'(\beta R s)} \quad (16)$$

and the transformed velocity potential is, from equation (6),

$$\bar{\varphi}(s; r, \theta) = -\frac{U_o}{\beta} \sum_0^{\infty} \frac{\bar{g}_m(s)}{s} \frac{K_m(\beta r s)}{K_m'(\beta R s)} \cos m\theta \quad (17)$$

In order to give the desired expression for  $\varphi(x, r, \theta)$  it is necessary to calculate the inverse Laplace transform of the functions  $K_m(\beta r s)/K_m'(\beta R s)$ . This task has been undertaken by Mersman (ref. 12).

**EXTERNAL WAVE DRAG OF QUASI-CYLINDRICAL BODY OF REVOLUTION IN TERMS OF ITS GEOMETRY OR SOURCE DISTRIBUTION**

Attention is now restricted to flow fields possessing axial symmetry with respect to the stream direction. Independence with respect to  $\theta$  then reduces equations (7) and (8) to

$$\varphi(x, r) = -\frac{1}{2\pi} \int_0^{x-\beta r} \frac{A_o(x_1) dx_1}{\sqrt{(x-x_1)^2 - \beta^2 r^2}} \quad (18)$$

and the velocity potential is expressed as a rectilinear distribution of supersonic source potentials. Operationally, equation (18) takes the form

$$\bar{\varphi}(s; r) = -\frac{1}{2\pi} \bar{A}_o(s) K_o(\beta r s) \quad (19)$$

The axes may now be considered as shifted so that the source distribution starts at  $x = -\beta R$  and induces perturbation velocities on the cylindrical surface  $r=R$ ,  $0 \leq x \leq l$ . For  $r \geq R$  one then has the disturbance field associated with a body of revolution that deviates only slightly from the cylinder  $r=R$ . The wave drag of such a body can then be expressed in two ways: first, as a function of the body geometry; second, as a function of the source-strength distribution. The first result has been given in reference 1. To the order of accuracy to which this control-surface theory applies, the slope of the resulting surface is

$$\frac{dr}{dx} \approx \frac{S'(x)}{2\pi R} \approx \frac{1}{U_o} \varphi_r \Big|_{r=R} \quad (20)$$

where  $S'(x)$  is the streamwise derivative of local cross-sectional area of the body. This condition, together with equation (19), yields

$$\frac{\bar{A}_o(s)}{U_o} = \frac{\bar{S}'(s)}{\beta R s K_1(\beta R s)} \quad (21)$$

where  $\bar{S}'(s)$  means the Laplace transform of  $S'(x)$ , and

$$\frac{\bar{\varphi}(s; R)}{U_o} = -\frac{\bar{S}'(s)}{2\pi \beta R s} \frac{K_o(\beta R s)}{K_1(\beta R s)} \quad (22)$$

In order to calculate drag, pressure on the body is next evaluated. Denoting by  $p$  and  $p_o$  local and free-stream pressure and setting  $q_o = \frac{1}{2} \rho_o U_o^2$ , one has in linearized theory

$$\frac{p-p_o}{q_o} \Big|_{r=R} = -\frac{2u(x, R)}{U_o} \quad (23)$$

From equation (22)

$$\begin{aligned} \frac{\bar{u}(s; R)}{U_o} &= -\frac{1}{2\pi \beta R} \frac{\bar{S}'(s)}{s} \frac{K_o(\beta R s)}{K_1(\beta R s)} \\ &= -\frac{\bar{S}'(s)}{2\pi \beta R} \left[ 1 - \frac{K_1(\beta R s) - K_o(\beta R s)}{K_1(\beta R s)} \right] \end{aligned} \quad (24)$$

The inverse transform of the second term involving the Bessel function leads to the function  $W(x)$  introduced by Lighthill (ref. 2). By definition, its transform is

$$\bar{W}(s) = \frac{K_1(s) - K_o(s)}{K_1(s)} \quad (25)$$

Pressure distribution on the body can then be calculated from the expression

$$\frac{p-p_o}{q_o} = \frac{1}{\pi \beta R} \left[ S'(x) - \int_0^{x-\beta R} S'(x_1) W\left(\frac{x-x_1}{\beta R}\right) \frac{dx_1}{\beta R} \right] \quad (26)$$

The function  $W(x)$  is shown in figure 1; tabular values for  $-2 < x < 10$  are given in reference 1.

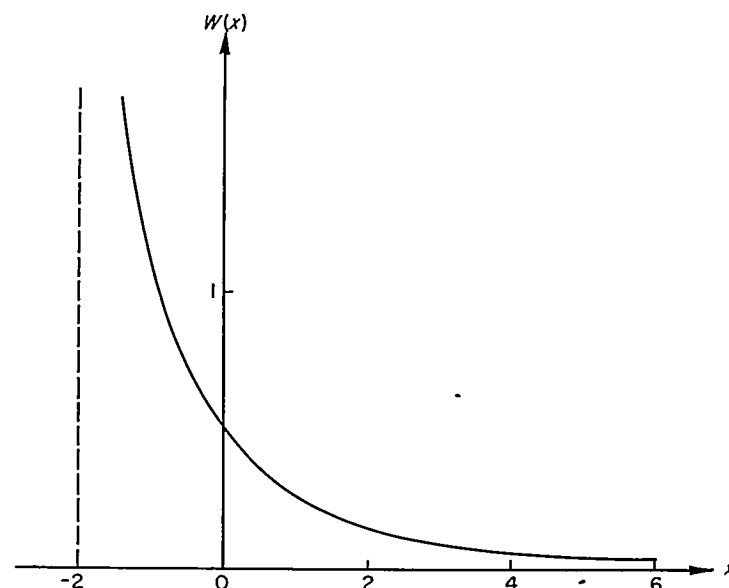


FIGURE 1.—The influence function  $W(x)$ .

The external wave drag  $C_{D_o}$  of the body is finally determined by direct integration

$$C_{D_o} = \frac{\text{drag}}{\pi R^2 q_0} = \frac{1}{\pi R^2} \int_0^l \frac{p-p_0}{q_0} S'(x) dx \quad (27)$$

and from equation (26) is

$$C_{D_o} = \frac{1}{2\beta\pi^2 R^3} \left\{ 2 \int_0^l [S'(x)]^2 dx - \frac{1}{\beta R} \int_0^l \int_0^l S'(x) S'(x_1) W\left(\frac{|x-x_1|}{\beta R}\right) dx dx_1 \right\} \quad (28)$$

In a later section entitled "Geometric Criteria for Minimum Drag," the role equation (28) plays in problems involving drag minimization will be discussed. For the present, it may be remarked that although the magnitude of the influence function  $W(x)$  is known, its analytic properties are not well enough defined to permit easy manipulation. It will become more apparent later that for certain minimum-drag problems an advantage is provided when one deals directly with source distributions and establishes the relationship between geometry and source strengths as a separate part of the analysis.

Equation (18) expresses the potential of a source distribution of strength  $A_o(x)$ . On the cylindrical control surface  $r=R$  and within the range  $0 \leq x \leq l$  an effective body shape is induced and the drag of this body can be calculated as follows. The streamwise and lateral perturbation-velocity components are, respectively,

$$\varphi_x(x, r) = -\frac{1}{2\pi} \int_{-\beta R}^{x-\beta R} \frac{A_o'(x_1) dx_1}{\sqrt{(x-x_1)^2 - \beta^2 r^2}} \quad (29)$$

$$\varphi_r(x, r) = \frac{1}{2\pi r} \int_{-\beta R}^{x-\beta R} \frac{(x-x_1) A_o'(x_1) dx_1}{\sqrt{(x-x_1)^2 - \beta^2 r^2}} \quad (30)$$

where  $A_o(x_1) = 0$  for  $x_1 \leq -\beta R$ . The effective body, within the range  $0 \leq x \leq l$ , is fixed by the boundary conditions of equation (20) and its external wave drag is

$$D = -2\pi \rho_0 R \int_0^l \varphi_x(x, R) \varphi_r(x, R) dx \\ = \frac{\rho_0}{2\pi} \int_0^l dx \int_{-\beta R}^{x-\beta R} \frac{A_o'(x_1)(x-x_1) dx_1}{\sqrt{(x-x_1)^2 - \beta^2 R^2}} \int_{-\beta R}^{x-\beta R} \frac{A_o'(x_2) dx_2}{\sqrt{(x-x_2)^2 - \beta^2 R^2}} \quad (31)$$

The dummy variables  $x_1, x_2$  can be interchanged; if one then combines the two expressions of equation (31) and inverts the order of integration,<sup>3</sup> the integration with respect to  $x$  can be performed and there results

$$D = \frac{\rho_0}{4\pi} \int_{-\beta R}^{l-\beta R} A_o'(x_1) dx_1 \int_{-\beta R}^{l-\beta R} A_o'(x_2) \cosh^{-1} \left| \frac{(l-x_1)(l-x_2) - \beta^2 R^2}{\beta R(x_1-x_2)} \right| dx_2 \quad (32)$$

as given in reference 3.

It is of interest to remark that although equation (32) uses only a knowledge of the function  $A_o(x)$  in the range  $-\beta R \leq x \leq l - \beta R$ , the drag that is calculated presupposes a

specific source distribution function in the range  $l - \beta R < x$  if one wishes to identify the drag with a geometric shape. Thus, as in figure 2, if the body shape near  $r=R$  is assumed to have some arbitrary variation for  $0 \leq x \leq l$ , and to straighten out into a purely cylindrical surface downstream of  $x=l$ , a source distribution function is required downstream of  $x=l - \beta R$  to produce the cylinder.

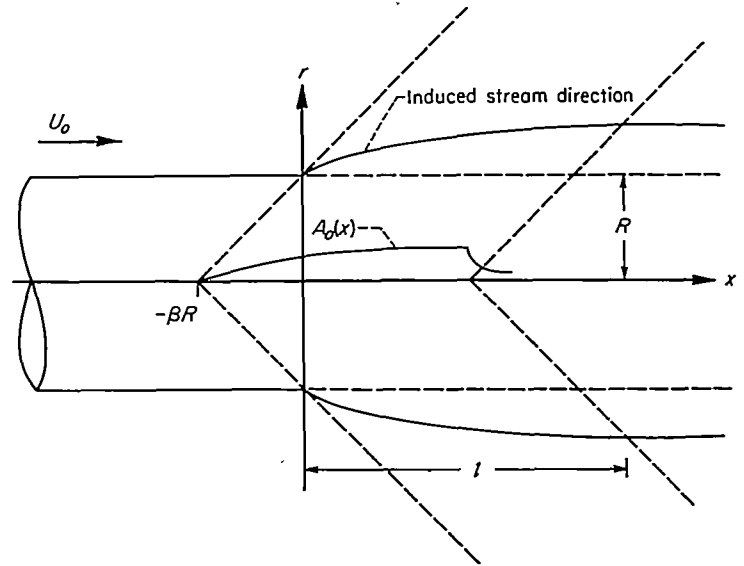


FIGURE 2.—Body induced on a control surface by an axial source distribution.

The fact that the stream velocity is supersonic means that upstream influences of  $A_o(x)$  for  $x > l - \beta R$  cannot be felt on the body and explains why the drag of a complete geometric shape can be determined from its source distribution without knowing the complete details of the distribution function.

As another example of the use of equation (32) consider, as in figure 3, a circular body extending from  $x = -\beta R$  to  $x = l$  with a cylindrical afterbody of radius  $R$  aft of  $x = l$ . If the source distribution of this body is known as, say, for example, in the case of a cone or slender body of revolution, the body drag can be determined by using the surface  $r=R, 0 \leq x \leq l$  as a control surface and calculating momen-

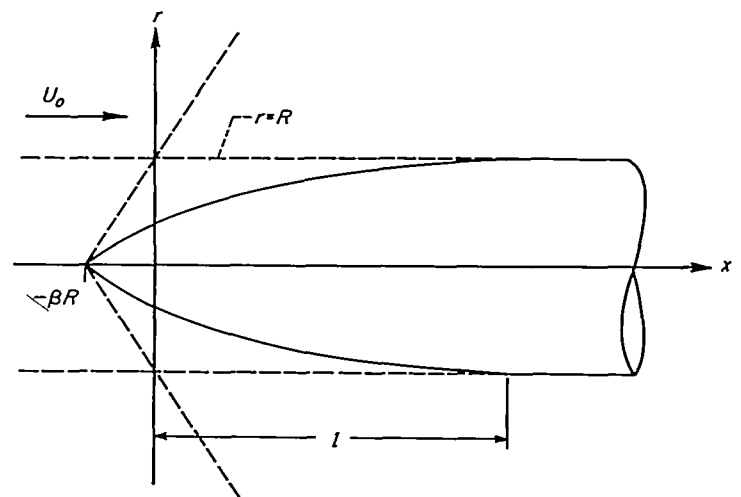


FIGURE 3.—Body nose induced by an axial source distribution.

<sup>3</sup>The inversion of order is permissible only if  $A_o(x)$  is suitably well behaved, a point that will arise later in the determination of the optimum body with given caliber.

tum transport through the control surface. Equation (32) is the exact expression for the body drag, and, again, requires no knowledge of source strength beyond  $x=l-\beta R$ .

**COMBINED FLOW FIELDS**

One method of attack that has proved to be extremely helpful in the analysis of problems in aerodynamic theory involves a symmetrization process in which flow fields in both forward and reverse flow are related. Attention, up to the present time, has been devoted principally to planar-type problems and in reference 13 Jones has used this approach to derive criteria that appear in the minimization of wave drag of, for example, nonlifting wings having specified thickness ratios or volumes. In this section, a brief discussion is given, using the methods of reference 14, of the way these concepts appear in cylindrical-control-surface analysis.

**THE RECIPROCITY RELATION FOR AXIAL FLOW**

Equation (1) can be written

$$L(\varphi) \equiv \beta^2 \varphi_{xx} - \varphi_{yy} - \varphi_{zz} = 0 \quad (33)$$

where  $L(\varphi)$  is a self-adjoint linear operator. Let now  $\psi(x,y,z)$  and  $\Omega(x,y,z)$  be two solutions of equation (33) satisfying boundary conditions given on a circular cylinder. Reciprocal relations between  $\psi$  and  $\Omega$  can be derived by applying Green's theorem over a prescribed geometric region. Consider, as shown in figure 4, the cylindrical control surface extending from  $x=0$  to  $x=l$  and draw the enveloping Mach cones at the front and rear of the surface.

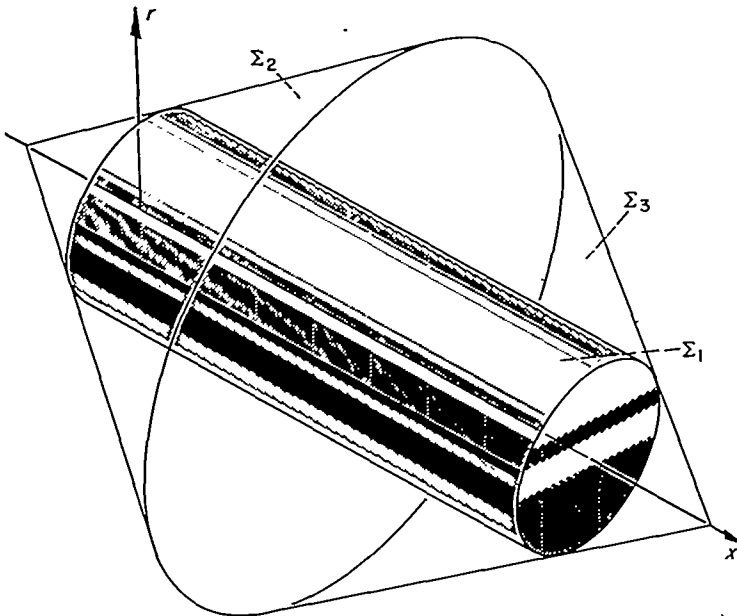


FIGURE 4.—Surfaces of integration for combined-flow analysis.

Denote the cylindrical surface by  $\Sigma_1$ , the front Mach cone  $x-\beta r=-\beta R$  by  $\Sigma_2$ , and the rear cone  $x+\beta r=l+\beta R$  by  $\Sigma_3$ . These surfaces enclose a toroidal region, bounded internally by  $\Sigma_1$  and externally by  $\Sigma_2$  and  $\Sigma_3$ . It follows from Green's theorem that the integral relation

$$\begin{aligned} \iint \psi \left( -\beta^2 n_1 \frac{\partial \Omega}{\partial x} + n_2 \frac{\partial \Omega}{\partial y} + n_3 \frac{\partial \Omega}{\partial z} \right) d\Sigma \\ = \iint \Omega \left( -\beta^2 n_1 \frac{\partial \psi}{\partial x} + n_2 \frac{\partial \psi}{\partial y} + n_3 \frac{\partial \psi}{\partial z} \right) d\Sigma \end{aligned} \quad (34)$$

applies where the surface integration extends over  $\Sigma_1, \Sigma_2, \Sigma_3$  and  $n_1, n_2, n_3$  are direction cosines, with respect to the  $x, y, z$  axes, of the surface normal directed inward into the region.

It is customary to re-express relations like equation (34) in terms of a newly defined directional derivative along a line termed the conormal. In this manner, the equation becomes

$$\iint \psi \Lambda \frac{\partial \Omega}{\partial v} d\Sigma = \iint \Omega \Lambda \frac{\partial \psi}{\partial v} d\Sigma \quad (35)$$

where

$$\frac{\partial \varphi}{\partial v} = \frac{\partial \varphi}{\partial x} v_1 + \frac{\partial \varphi}{\partial y} v_2 + \frac{\partial \varphi}{\partial z} v_3 \quad (36)$$

and the direction cosines  $v_1, v_2, v_3$  of the conormal are derived from

$$-n_1 \beta^2 = \Lambda v_1, \quad n_2 = \Lambda v_2, \quad n_3 = \Lambda v_3$$

By calculation of the respective normals  $n_1, n_2, n_3$  and using the relation  $v_1^2 + v_2^2 + v_3^2 = 1$ , it is readily found from the equations defining the conormal that on the surface  $\Sigma_1$ , the conormal is normal to the surface and  $\Lambda=1$ ; on a Mach cone, the conormal lies along the cone and  $\Lambda=\beta$

Let now  $\psi$  be set equal to  $\varphi(x, r, \theta)$ , the perturbation velocity potential associated with boundary conditions in a forward-flowing stream, and let  $\Omega$  be  $\tilde{u}(x, r, \theta)$ , the  $x$ -wise component of perturbation velocity associated with boundary conditions in a stream flowing in the reverse direction. Under these conditions, equation (35) becomes

$$\begin{aligned} \int_0^{2\pi} R d\theta \int_0^l \tilde{u} \frac{\partial \varphi}{\partial r} dx + \beta \iint \tilde{u} \frac{\partial \varphi}{\partial v} d\Sigma_2 + \beta \iint \tilde{u} \frac{\partial \varphi}{\partial v} d\Sigma_3 \\ = \int_0^{2\pi} R d\theta \int_0^l \varphi \frac{\partial \tilde{u}}{\partial r} dx + \beta \iint \varphi \frac{\partial \tilde{u}}{\partial v} d\Sigma_2 + \beta \iint \varphi \frac{\partial \tilde{u}}{\partial v} d\Sigma_3 \end{aligned}$$

On the Mach cone  $\Sigma_2$ , the perturbation potential may arbitrarily be set equal to zero and its conormal derivative along the cone will also be zero; as a consequence, the second terms on both sides of the equation vanish. Since the flow fields are irrotational,  $\partial \tilde{u} / \partial r = \partial \tilde{v}_r / \partial x$  where  $v_r$  is radial velocity. After making this substitution and integrating the first term in the right member by parts, one gets

$$\begin{aligned} R \int_0^{2\pi} d\theta \int_0^l \tilde{u} v_r dx = R \int_0^{2\pi} \left[ \varphi(l, R, \theta) \tilde{v}_r(l, R, \theta) - \int_0^l \tilde{v}_r u dx \right] d\theta - \\ \beta \int_0^{2\pi} d\theta \int_{x=l/2}^{x=l} r \left( \tilde{u} \frac{\partial \varphi}{\partial v} - \varphi \frac{\partial \tilde{u}}{\partial v} \right) dv \end{aligned}$$

The last integral becomes

$$-\beta \int_0^{2\pi} d\theta \int_{x=l/2}^{x=l} (\sqrt{r} \tilde{u})^2 \frac{d}{dv} \left( \frac{\varphi}{\tilde{u}} \right) dv$$

and for the given boundary conditions it is possible to show that along a conormal of  $\Sigma_3$  the relation  $\tilde{v}_r = \beta \tilde{u}$  holds and

$\sqrt{r} \tilde{u}$  is independent of  $\nu$ . The integral then can be rewritten as

$$\beta \int_0^{2\pi} d\theta \int_{x=l/2}^{x=l} (\sqrt{r} \tilde{u})^2 \frac{d}{d\nu} \left( \frac{\varphi}{\tilde{u}} \right) d\nu = \beta R \int_0^{2\pi} \tilde{u}(l, R, \theta) \varphi(l, R, \theta) d\theta$$

and one has, finally, the desired reciprocal theorem

$$-R \int_0^{2\pi} d\theta \int_0^l \tilde{u}(x, R, \theta) v_r(x, R, \theta) dx = R \int_0^{2\pi} d\theta \int_0^l u(x, R, \theta) \tilde{v}_r(x, R, \theta) dx \quad (37)$$

It is not the purpose here to exploit the various applications of equation (37); rather, the role played by the reciprocal relation in drag calculations will be considered. In the forward and reverse flow fields, the pressure-velocity relations of linearized theory are

$$p - p_0 = -\rho_0 U_0 u, \quad \tilde{p} - p_0 = \rho_0 U_0 \tilde{u} \quad (38)$$

If, furthermore, thickness distributions of the form

$$r = f(x, \theta), \quad r = \tilde{f}(x, \theta)$$

are placed on the cylinder  $r=R$ , the boundary conditions are

$$\left. \frac{1}{U_0} \frac{\partial \varphi}{\partial r} \right]_{r=R} = \frac{\partial f}{\partial x}, \quad \left. \frac{1}{U_0} \frac{\partial \tilde{\varphi}}{\partial r} \right]_{r=R} = -\frac{\partial \tilde{f}}{\partial x}$$

Equation (37) can then be written

$$-\int_0^{2\pi} R d\theta \int_0^l (\tilde{p} - p_0) \frac{\partial f}{\partial x} dx = \int_0^{2\pi} R d\theta \int_0^l (p - p_0) \frac{\partial \tilde{f}}{\partial x} dx \quad (39)$$

An immediate consequence of this last result is that for a unique thickness distribution, that is, for  $f(x, \theta) = \tilde{f}(x, \theta)$ , the drag of a body in forward and reverse flow is the same. This follows from the fact that for quasi-cylindrical bodies the relations for drag are, respectively,

$$D = R \int_0^{2\pi} d\theta \int_0^l (p - p_0)_{r=R} \frac{\partial f}{\partial x} dx$$

$$\tilde{D} = -R \int_0^{2\pi} d\theta \int_0^l (\tilde{p} - p_0)_{r=R} \frac{\partial \tilde{f}}{\partial x} dx$$

For fixed geometry, therefore, drag is equal to half the sum of these two expressions

$$D = \frac{R}{2} \int_0^{2\pi} d\theta \int_0^l (p - \tilde{p})_{r=R} \frac{\partial f}{\partial x} dx$$

Defining pressure  $P(x, r, \theta)$  in the combined flow fields by the following

$$P(x, r, \theta) = p - \tilde{p} = -\rho_0 U_0 (u + \tilde{u}) \quad (40)$$

one has

$$D = \frac{R}{2} \int_0^{2\pi} d\theta \int_0^l P(x, R, \theta) \frac{\partial f}{\partial x} dx \quad (41)$$

If the body has axial symmetry, equation (41) reduces to the form given in equation (28). To show this, one notes first that  $P$  and  $f$  are independent of  $\theta$  and that equation (41) becomes

$$D = \frac{1}{2} \int_0^l P S'(x) dx$$

The proof follows from the relations

$$\left. \begin{aligned} S'(x) &= \tilde{S}'(x) \\ \frac{u(x, R)}{U_0} &= -\frac{1}{2\pi\beta R} \left[ S'(x) - \int_0^x S'(x_1) W\left(\frac{x-x_1}{\beta R}\right) \frac{dx_1}{\beta R} \right] \\ \frac{\tilde{u}(x, R)}{U_0} &= -\frac{1}{2\pi\beta R} \left[ S'(x) + \int_x^l S'(x_1) W\left(\frac{x_1-x}{\beta R}\right) \frac{dx_1}{\beta R} \right] \\ \frac{P(x, R)}{q_0} &= \frac{1}{\pi\beta R} \left[ 2S'(x) - \int_0^l S'(x_1) W\left(\frac{|x-x_1|}{\beta R}\right) \frac{dx_1}{\beta R} \right] \end{aligned} \right\} \quad (42)$$

#### GEOMETRIC CRITERIA FOR MINIMUM DRAG

Consider now the problem of minimizing the wave drag of a quasi-cylindrical body subject to the condition that the volume of the body is constant. The body surface may be defined by

$$r = f(x, \theta) = R + g(x, \theta) \quad (43)$$

The function  $g(x, \theta)$  determines the magnitude of the surface displacement from the cylinder  $r=R$ ; these displacements, as well as their gradients, are assumed small and we also assume

$$g(x, \theta) \equiv 0 \text{ for } x \leq 0 \text{ and } l \geq x$$

If equation (41) is integrated by parts with respect to  $x$ , the wave drag of the body becomes

$$D = -\frac{R}{2} \int_0^{2\pi} d\theta \int_0^l P'(x, R, \theta) g(x, \theta) dx \quad (44)$$

where the prime indicates  $x$ -wise differentiation of  $P$ . The imposed geometric constraint on the variational problem is

$$\begin{aligned} \frac{1}{2} \int_0^{2\pi} d\theta \int_0^l f^2(x, \theta) dx &\approx \frac{1}{2} \int_0^{2\pi} d\theta \int_0^l [R^2 + 2Rg(x, \theta)] dx \\ &= \pi R^2 l + R \int_0^{2\pi} d\theta \int_0^l g(x, \theta) dx = V = \text{const.} \end{aligned} \quad (45)$$

where  $V$  is the total volume. The problem thus becomes one of minimizing the expression

$$D - \mu V = -R \left\{ \frac{1}{2} \int_0^{2\pi} d\theta \int_0^l P' g(x, \theta) dx + \mu \left[ \pi R l + \int_0^{2\pi} d\theta \int_0^l g(x, \theta) dx \right] \right\} \quad (46)$$

where  $\mu$  is the Lagrangian multiplier. Carrying out the variation, one has

$$\delta(D - \mu V) = -\frac{R}{2} \int_0^{2\pi} d\theta \int_0^l [P'(\delta g) + g(\delta P') + 2\mu \delta g] dx = 0$$

but from equation (37) or (39) it can be shown that the first two terms in the integrand yield equal integrals and the minimizing condition becomes

$$\int_0^{2\pi} d\theta \int_0^l [P'(x, R, \theta) + \mu] \delta g dx = 0$$

Since this latter equation must be satisfied by all possible variations of the displacement function  $g(x, \theta)$ , it follows that the desired condition is

$$P'(x, R, \theta) + \mu = 0 \quad (47)$$

Stated in words, the condition for minimum wave drag of a quasi-cylindrical body of given volume is that the longitudinal gradient of pressure on the body in the combined forward and reverse flow field is a constant. Furthermore, from equation (44), minimum drag is then given by

$$D_{min} = \frac{\mu}{2} (V - \pi R^2 l) = \frac{\mu}{2} V_e \quad (48)$$

where  $\mu$  can now be identified with the negative pressure gradient in the combined field and  $(V - \pi R^2 l) = V_e$  is the volume exposed to the fluid around the cylindrical control surface  $r = R$ .

The actual cross-section-area variation of a minimum-drag constant-volume body and its pressure distribution are shown in figure 5 for the case in which axial symmetry

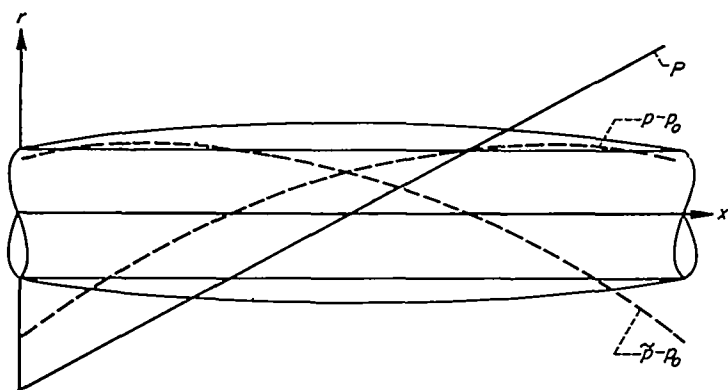


FIGURE 5.—Minimum drag body with pressure distributions in combined flow.

is imposed. Pressure coefficient in the combined flow field of an axially symmetric body has been given in equation (42). The geometric criterion just established then leads to the integral equation

$$2S'(x) - \int_0^l S'(x_1) W\left(\frac{|x-x_1|}{\beta R}\right) \frac{dx_1}{\beta R} = -\mu x + b \quad (49)$$

and the solution of this equation will determine the body geometry. In the following section an analogous integral equation will be derived but with the source-strength distribution chosen as the fundamental dependent variable.

The combined-flow-field technique can also be used to study the problem of minimizing wave drag for specified body caliber or, more generally, when the body has a fixed cross section at a specified longitudinal position. The resulting condition for minimum drag is that the pressure distribution on the body in the combined flow field is a constant forward and aft of the specified position. These conditions are all analogous to those obtained for planar problems by R. T. Jones (ref. 13).

### DRAG MINIMIZATION

In this division, optimum bodies having certain prescribed geometric properties will be determined by standard variational methods. The analysis will, as mentioned previously, deal with the strength of an axial source distribution as the minimizing function, rather than the geometric quantity,

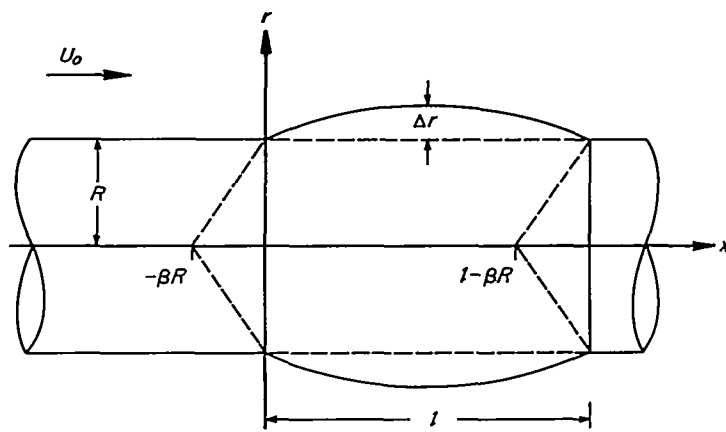


FIGURE 6.—Body and associated nomenclature used in drag minimization.

cross-sectional area. Thus, we shall be concerned with formula (32), giving drag in terms of the source distribution.

#### QUASI-CYLINDRICAL BODY OF REVOLUTION OF GIVEN VOLUME

**Isoperimetric conditions.**—The configuration to be considered, together with associated nomenclature, is shown in figure 6. The geometric properties of the body can be expressed in terms of the source distribution function  $A_o(x)$  by using equation (20), namely,

$$S'(x) = \frac{2\pi R}{U_o} \varphi_r \Big|_{r=R} \quad (50)$$

Then, from equation (30)

$$S'(x) = \frac{1}{U_o} \int_{-\beta R}^{x-\beta R} \frac{A_o'(x_1)(x-x_1)}{\sqrt{(x-x_1)^2 - \beta^2 R^2}} dx_1 \quad (51)$$

If equation (51) is integrated  $x$ -wise it is seen that

$$S(x) - S(o) = \frac{1}{U_o} \int_0^x dz \int_{-\beta R}^{z-\beta R} \frac{(z-x_1)A_o'(x_1)dx_1}{\sqrt{(z-x_1)^2 - \beta^2 R^2}} \quad (52a)$$

By changing the order of integration and performing the integration with respect to  $z$  one finds

$$S(x) - S(o) = \frac{1}{U_o} \int_{-\beta R}^{x-\beta R} \frac{(x-x_1)A_o(x_1)}{\sqrt{(x-x_1)^2 - \beta^2 R^2}} dx_1 \quad (52b)$$

or, integrating by parts,

$$S(x) - S(o) = \frac{1}{U_o} \int_{-\beta R}^{x-\beta R} A_o'(x_1) \sqrt{(x-x_1)^2 - \beta^2 R^2} dx_1 \quad (52c)$$



The magnitude of the additional volume wrapped around the cylinder is

$$V_e = \int_0^l [S(x) - S(0)] dx \quad (53a)$$

and, from equation (52b),

$$V_e = \frac{1}{U_o} \int_{-\beta R}^{l-\beta R} A_o(x_1) \sqrt{(l-x_1)^2 - \beta^2 R^2} dx_1 \quad (53b)$$

The variational problem.—The quantity to be minimized will be taken as  $D - \mu_1 V_e$ . From equation (32), the drag can be written, after an integration by parts,

$$D = \frac{\rho_o}{4\pi} \int_{-\beta R}^{l-\beta R} \frac{A_o(x_1) dx_1}{\sqrt{(l-x_1)^2 - \beta^2 R^2}} - \int_{-\beta R}^{l-\beta R} \frac{A_o'(x_2) \sqrt{(l-x_2)^2 - \beta^2 R^2}}{x_1 - x_2} dx_2 \quad (54)$$

In addition to prescribing the volume added to the fundamental cylinder, we shall also require that the body return at the end to the same cross-sectional area as at the front. Thus, according to equation (52b),

$$0 = \int_{-\beta R}^{l-\beta R} \frac{(l-x_1) A_o(x_1) dx_1}{\sqrt{(l-x_1)^2 - \beta^2 R^2}} \quad (55)$$

$$A_o'(x) \sqrt{(l-x)^2 - \beta^2 R^2} = \frac{1}{\pi \sqrt{(l-\beta R-x)(x+\beta R)}} \left\{ \pi \int_{-\beta R}^{l-\beta R} A_o'(x_1) \sqrt{(l-x_1)^2 - \beta^2 R^2} dx_1 - \int_{-\beta R}^{l-\beta R} \frac{\lambda(l-x_1) + \frac{2\pi\mu_1}{\rho_o U_o} [(l-x_1)^2 - \beta^2 R^2]}{x-x_1} \sqrt{(l-\beta R-x_1)(x_1+\beta R)} dx_1 \right\}$$

The first integral on the right vanishes according to the closure condition (55) and, if the remaining integrations are performed, we find

$$A_o'(x) \sqrt{(l-x)^2 - \beta^2 R^2} = \frac{1}{\pi \sqrt{(l-\beta R-x)(x+\beta R)}} \left\{ \frac{l(l+4\beta R)}{16} \left( \frac{2\pi l}{\rho_o U_o} \mu_1 + 2\lambda \right) + \frac{l-\beta R-x}{8} \left[ 4\lambda(l-2x) + \frac{2\pi\mu_1}{\rho_o U_o} (3l^2 - 4\beta Rl - 8\beta^2 R^2 - 12lx + 8x^2) \right] \right\}$$

It will be noted that unless

$$\frac{2\pi l}{\rho_o U_o} \mu_1 + 2\lambda = 0$$

this solution for  $A_o'(x)$  does not obey the closure requirement. Therefore we impose this last condition and finally obtain

$$A_o'(x) = \frac{\mu_1}{4\rho_o U_o} \frac{(l^2 - 4\beta Rl - 8\beta^2 R^2) - 8lx + 8x^2}{\sqrt{(l+\beta R-x)(x+\beta R)}} \quad (57)$$

The strength of the minimizing source distribution  $A_o(x)$  is now obtained by integrating equation (57);

$$A_o(x) = \frac{\mu_1}{2\rho_o U_o} \left[ (l-2x) \sqrt{(l+\beta R-x)(x+\beta R)} - 2\beta^2 R^2 \cos^{-1} \frac{l-2x}{l+2\beta R} \right] \quad (58a)$$

is a condition to be met by the minimizing function  $A_o(x_1)$ , and by its variations.

The quantity  $D - \mu_1 V_e$  can be formed from equations (53) and (54), and if the variation is performed, one finds the condition

$$\int_{-\beta R}^{l-\beta R} \frac{\delta A_o(x_1) dx_1}{\sqrt{(l-x_1)^2 - \beta^2 R^2}} \left\{ \int_{-\beta R}^{l-\beta R} \frac{A_o'(x_2) \sqrt{(l-x_2)^2 - \beta^2 R^2}}{x_1 - x_2} dx_2 - \frac{2\pi}{\rho_o U_o} \mu_1 [(l-x_1)^2 - \beta^2 R^2] \right\} = 0$$

If this last equation is compared with equation (55), it is seen that for admissible variations, the quantity within the brackets must be set equal to  $\lambda(l-x_1)$ , where  $\lambda$  is an arbitrary constant. Thus, the equation for determination of the optimizing source distribution under the conditions of given volume and closure is

$$\int_{-\beta R}^{l-\beta R} \frac{A_o'(x_1) \sqrt{(l-x_1)^2 - \beta^2 R^2}}{x-x_1} dx_1 = \lambda(l-x) + \frac{2\pi\mu_1}{\rho_o U_o} [(l-x)^2 - \beta^2 R^2] \quad (56)$$

Equation (56) is recognized as the familiar airfoil equation with  $[A_o'(x_1) \sqrt{(l-x_1)^2 - \beta^2 R^2}]$  as the unknown. Thus we write the solution immediately as (see, e.g., ref. 15)

Properties of the optimal source distribution.—It is convenient to express the various quantities such as source strength, area distribution, etc., as dimensionless functions of the dimensionless variable  $\eta = x/l$  and parameter  $\sigma = \beta R/l$ . Thus, indicating a dimensionless function by a star, we have from equation (58a)

$$A_o^*(\eta) = \frac{A_o(l\eta)}{lU_o} = \frac{l\mu_1}{4q_o} \left[ (1-2\eta) \sqrt{(\eta+\sigma)(1-\eta+\sigma)} - 2\sigma^2 \cos^{-1} \frac{1-2\eta}{1+2\sigma} \right] \quad (58b)$$

It will be noted that if the radius of the control surface is taken very small, so that  $\sigma \rightarrow 0$ , formula (58b) becomes

$$A_o^*(\eta) |_{\sigma \rightarrow 0} = \frac{\mu_1 l}{4q_o} (1-2\eta) \sqrt{\eta(1-\eta)}$$

which is the well-known slender-body theory result for the source distribution corresponding to an optimum body of given volume (refs. 16 and 17.)

In order to determine the value of the Lagrange multiplier  $\mu_1$ , in terms of the prescribed volume  $V_e$ , it is convenient to find first the expression for the local cross-section area of the optimum body. Thus, using equation (52c) (with  $S^*(\eta) = \frac{1}{l^2} S(l\eta)$ ),

$$S^*(\eta) - S^*(0) = \frac{\mu_1 l}{6q_0} \sqrt{(\eta+2\sigma)(1-\eta+2\sigma)} [\eta(1-\eta)E - \sigma(1-4\sigma)(K-E)] \quad (59)$$

where  $K$  and  $E$  are elliptic integrals of the first and second kinds, respectively, of modulus

$$k^2 = \frac{\eta(1-\eta)}{(\eta+2\sigma)(1-\eta+2\sigma)}$$

Using equation (59) in equation (53a), we find

$$V_e^* = \frac{\mu_1 l}{6q_0} \int_0^1 \sqrt{(\eta+2\sigma)(1-\eta+2\sigma)} [\eta(1-\eta)E - \sigma(1-4\sigma)(K-E)] d\eta = \frac{\mu_1 l}{6q_0} B(\sigma) \quad (60a)$$

which expresses the constant  $\mu_1$ , in terms of the prescribed volume  $V_e^*$  ( $= \frac{V_e^*}{l^3}$ ) and of a function  $B$  of the quantity  $\sigma = \beta R/l$ . A graph of this function  $B(\sigma)$  versus  $\sigma$  is shown in

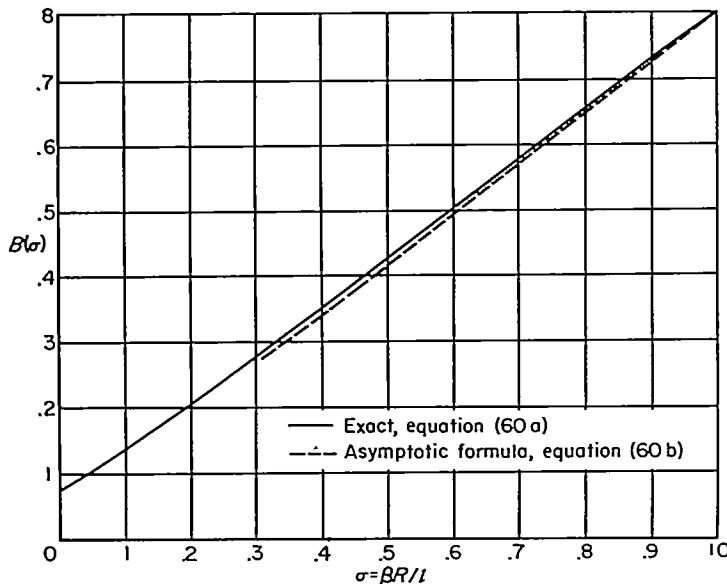


FIGURE 7.—The function  $B(\sigma)$ .

figure 7. Shown also in figure 7 is a dashed line that corresponds to the asymptotic form for  $B(\sigma)$ , which is

$$B(\sigma) \sim \frac{\pi}{16} (1+4\sigma) \sqrt{\frac{2\sigma}{1+2\sigma}} \quad (60b)$$

The closeness of the asymptotic values to the exact values even for relatively small values of  $\sigma$  is noteworthy.

The formulae (58b) and (59) for the source strength and cross-section area, respectively, can now be recast in terms of prescribed quantities

$$A_o^*(\eta) = \frac{3}{2} \frac{V_e^*}{B(\sigma)} \left[ (1-2\eta) \sqrt{(\eta+\sigma)(1-\eta+\sigma)} - 2\sigma^2 \cos^{-1} \frac{1-2\eta}{1+2\sigma} \right] \quad (61)$$

$$\frac{S^*(\eta) - S^*(0)}{S^*(0)} = \frac{(V_e^*/V_o^*)}{B(\sigma)} \sqrt{(\eta+2\sigma)(1-\eta+2\sigma)} [\eta(1-\eta)E - \sigma(1-4\sigma)(K-E)] \quad (62a)$$

where  $V_o$  is the volume of the original cylinder section,

$$V_o = \pi R^2 l = l S(0) = l^3 V_o^*$$

Consider the expression (61) for the source function  $A_o^*(\eta)$ . In the parameter  $\sigma = \beta R/l$ , we may think of  $\beta$  as fixed and  $l$  as unity, so that variations in  $\sigma$  amount to variations in the size of the control surface of radius  $R$ . Thus, in figure 8, the

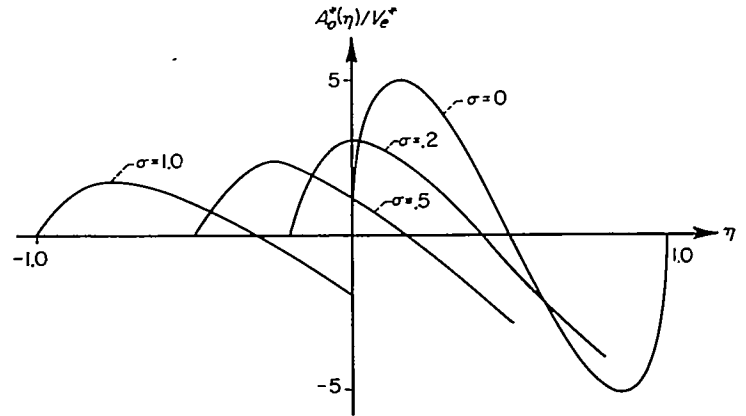


FIGURE 8.—Optimum source distributions for various values of the parameter  $\sigma$ .

case  $\sigma = 0$  corresponds to the source distribution for the well-known Sears-Haack body (refs. 16 and 17). It will be noted in the cases where  $\sigma > 0$  that the source functions become less steep and attain lesser maximum values because the volume remains the same while the control-surface cylinder is increasing, thus giving a smaller maximum radius of the added portion.

Next let us examine the expression (62a) for cross-sectional area. First, we notice that it can be written

$$S^*(\eta) - S^*(0) = \frac{V_e^*}{B(\sigma)} \sqrt{(\eta+2\sigma)(1-\eta+2\sigma)} [\eta(1-\eta)E - \sigma(1-4\sigma)(K-E)] \quad (62b)$$

in which form it reduces formally for  $\sigma \rightarrow 0$  to

$$S^*(\eta) = \frac{128}{3\pi} V_e^* [\eta(1-\eta)]^{3/2} \quad (62c)$$

which is identical with the expression for cross-section area of a slender optimum body of prescribed volume (Sears-Haack body). Of course,  $V_e$  is, in this case, the total volume of the body. On the other hand, if we allow the radius of the control surface to increase indefinitely, equation (62b) gives (using the asymptotic form for  $B(\sigma)$ , eq. (60b))

$$S^*(\eta) - S^*(0) = 6V_e^* \eta(1-\eta)$$

In the case when  $R$  is very large, we take

$$S(x) - S(0) = 2\pi R \Delta r(x) \quad (63)$$

so we have, returning to the original variables,

$$\Delta r(x) = 6 \frac{V_e}{2\pi R l} \frac{x(l-x)}{l^2} \quad (64)$$

where  $V_e/2\pi R l$  is a finite quantity, and, in fact, is the average height of the protuberance above the control cylinder. This

result is clear from physical reasoning, for one would expect that as the control cylinder increased in radius, the two-dimensional result for the optimum problem would become more nearly valid, and, indeed, equation (64) is the formula for a two-dimensional biconvex section, where  $\Delta r$  is distance from the mean line,  $l$  is chord length, and maximum thickness is  $\left(\frac{3}{4} \frac{V_0}{\pi R l}\right)$ .

It will be noted that the area distribution as given by equation (62b) has fore-and-aft symmetry, since the functional dependence upon  $\eta$  involves only the combination  $\eta(1-\eta)$ . The maximum cross-section of the optimum body then occurs at the midpoint  $\eta = \frac{1}{2}$  and is given by (from eq. (62b))

$$S^*_{max} - S^*(0) = 2V_0^* \frac{1+4\sigma}{4B(\sigma)} \left[ \frac{E}{4} - \sigma(1-4\sigma)(K-E) \right] = 2V_0^* T(\sigma) \quad (65)$$

where the modulus of the elliptic integrals is now  $k = 1/(1+4\sigma)$ . Figure 9 shows the function  $T(\sigma)$  versus  $\sigma$ .

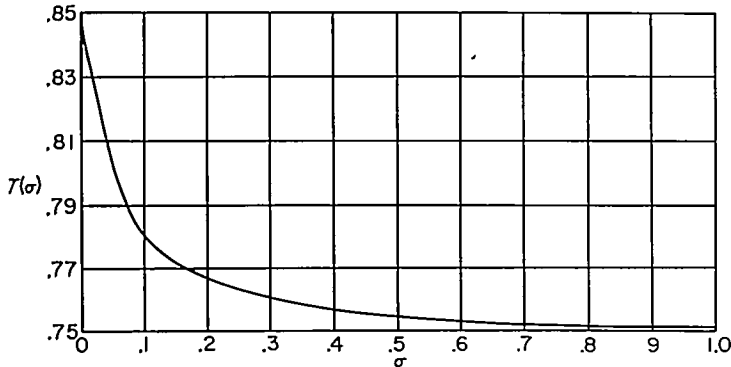


FIGURE 9.—The function  $T(\sigma)$ .

The drag of the optimum bodies can now be evaluated. From equations (54) and (56)

$$D = \frac{\rho_0}{4\pi} \int_{-\beta R}^{l-\beta R} \frac{A_0(\xi) d\xi}{\sqrt{(l-\xi)^2 - \beta^2 R^2}} \left\{ \lambda(l-\xi) + \frac{2\pi\mu_1}{\rho_0 U_0} [(l-\xi)^2 - \beta^2 R^2] \right\}$$

The integral involving  $\lambda$  vanishes because of the closure condition. The remaining integration gives

$$D = \frac{\mu_1}{2U_0} \int_{-\beta R}^{l-\beta R} A_0(\xi) \sqrt{(l-\xi)^2 - \beta^2 R^2} d\xi = \frac{\mu_1 V_0}{2} \quad (66)$$

by equation (53b). Finally, using the evaluation of  $\mu_1$  of equation (60a), we have

$$\frac{D}{q_0} = 3 \frac{V_0^2}{l^4 B(\sigma)} \quad (67)$$

$$\frac{S^*(\eta) - S^*(0)}{\Delta S^*} = \frac{2}{\pi(1+4\sigma)} \frac{(1+2\sigma)(1+4\sigma)\Pi(\alpha^2, k) - (1-2\eta)(\eta+2\sigma)(1-\eta+2\sigma)E - (1+2\sigma)(1-\eta+2\sigma)K}{\sqrt{(\eta+2\sigma)(1-\eta+2\sigma)}} \quad (71)$$

where  $\Pi(\alpha^2, k)$  is a complete elliptic integral of third kind of modulus  $k^2 = \frac{\eta(1-\eta)}{(\eta+2\sigma)(1-\eta+2\sigma)}$  and parameter  $\alpha^2 = \frac{-\eta}{1-\eta+2\sigma}$ .

Again  $K$  and  $E$  are complete elliptic integrals of the first and second kinds, respectively, of the same modulus  $k$ .

If we allow  $\sigma$  to approach zero, equation (71) becomes, in the limit,

Numerical results pertaining to the problem just solved will be given in a later section, and a summary of the important formulae is given in the appendix.

#### QUASI-CYLINDRICAL BODY OF REVOLUTION WITH GIVEN CALIBER

**The variational problem.**—For this problem, we prescribe the area at the base of the body, so the given condition is, from equation (52b)

$$\Delta S = S(l) - S(0) = \frac{1}{U_0} \int_{-\beta R}^{l-\beta R} \frac{(l-x_1)A_0(x_1)dx_1}{\sqrt{(l-x_1)^2 - \beta^2 R^2}} \quad (68)$$

The variation can be taken as before (now without invoking the closure condition) on the quantity  $D + \lambda \Delta S$ , and it leads to the integral equation

$$\int_{-\beta R}^{l-\beta R} \frac{A_0'(x_1) \sqrt{(l-x_1)^2 - \beta^2 R^2}}{x-x_1} dx_1 = -\frac{2\pi\lambda}{\rho_0 U_0} (l-x) \quad (69)$$

The solution to equation (69) can be written immediately by analogy with that for equation (56). The presence of a linear singularity in  $A_0'(x)$  must be disallowed, however, according to a condition mentioned in deriving the drag formula, equation (32). Thus, we have here to set

$$\lambda = -\frac{8q_0 \Delta S}{\pi l(l+4\beta R)}$$

and the solution consistent with the given conditions is

$$A_0'(x) = \frac{4}{\pi} \frac{U_0(\Delta S)}{l(l+4\beta R)} \frac{l-2x}{\sqrt{(l+\beta R-x)(x+\beta R)}} \quad (70a)$$

Integrating this expression, we find for the strength of the optimizing source distribution

$$A_0(x) = \frac{8}{\pi} \frac{U_0(\Delta S)}{l(l+4\beta R)} \sqrt{(l+\beta R-x)(x+\beta R)} \quad (70b)$$

The source distribution of equation (70b) represents the first approximation to the result of reference 3 for nearly equal front and rear radii.

**Properties of the solution.**—As in the section on the body with prescribed volume, we now consider  $x$  made dimensionless by division by  $l$ , and again set  $\sigma = \beta R/l$ . The various quantities of interest in connection with the caliber problem then become

$$A_0^*(\eta) = \frac{8}{\pi} \frac{\Delta S^*}{1+4\sigma} \sqrt{(\eta+\sigma)(1-\eta+\sigma)} \quad (70c)$$

$$\frac{S^*(\eta)}{S^*(1)} = \frac{2}{\pi} [\sin^{-1} \sqrt{\eta} - (1-2\eta)\sqrt{\eta(1-\eta)}] \quad (72)$$

which is the shape function for the well-known Kármán ogive (ref. 18). At the other limit, when  $\sigma \rightarrow \infty$ , equation (71) gives (in the original variables)

$$\frac{S(x) - S(0)}{\Delta S} = \frac{x}{l}$$

or, using the approximation of equation (63),

$$\frac{\Delta r(x)}{\Delta r(l)} = \frac{x}{l} \quad (73)$$

which is again the expected two-dimensional result for specified caliber.

The drag can be found by substituting equation (69) in equation (54), and then using equation (52b). There results

$$\frac{D}{q_0} = \frac{4}{\pi(1+4\sigma)} \frac{(\Delta S)^2}{l^2} \quad (74)$$

A summary of formulae pertaining to this body will be found in the Appendix.

**EXAMPLES OF OPTIMUM BODIES**

**The optimum body of given volume.**—In order to examine in detail the dependence of the body geometry on the parameter  $\sigma$ , we may return to equation (62a). The quantity  $[S^*(\eta) - S^*(0)]$  is actually the local cross-sectional area added to the basic cylinder by the action of the source distribution. In figure 10 are shown some cases of optimum bodies, having equal additional volume  $V_e^*$ , for several values of the parameter  $\sigma$ . Only half of each distribution is shown, since they are symmetric about the point  $\eta=1/2$ . The one labeled  $\sigma=0$  is the Sears-Haack optimum body, and it will be noted that as  $\sigma$  increases, the curves depart rather quickly from this limiting case and approach the other limiting value of the biconvex distribution for  $\sigma \rightarrow \infty$ . In fact, a biconvex arc drawn through the end points of the  $\sigma=1/2$  case is indistinguishable from the exact result in the scale used. In the inset of figure 10 is shown the variation of the drag of the optimum bodies as a function of  $\sigma$ . This drag is also based on equal volume, and shows a fairly rapid decrease with increasing values of  $\sigma$ , due to the decrease in the thickness of the exposed portion of the body. The dashed curve on

the drag plot is the calculated drag  $\left[ \frac{D}{q_0(V_e/l^2)^2} = \frac{12}{\pi\sigma} \right]$  under the assumption that each meridian section of the body acts as an independent two-dimensional optimum airfoil. This admittedly crude approximation is of course very poor at low values of  $\sigma$ , but its accuracy becomes surprisingly good for  $\sigma$  greater than about 0.4, and the approximation becomes exact in the limit  $\sigma \rightarrow \infty$ .

The variation of local cross section with  $\sigma$  can be examined also on the basis of equal exposed area. Thus, using equation (65) in combination with equation (62b), we have

$$\frac{\Delta S^*(\eta)}{\Delta S^*_{max}} = \frac{1}{2T(\sigma)B(\sigma)} \sqrt{(\eta+2\sigma)(1-\eta+2\sigma)} \quad (75)$$

$$[\eta(1-\eta)E - \sigma(1-4\sigma)(K-E)]$$

Figure 11 shows plots of equation (75), and it is again noted that the departure from the slender-body approximation ( $\sigma=0$ ) is rapid. The limiting variation of area for  $\sigma \rightarrow \infty$  is also shown in figure 11, and it is seen again how closely the optimum body-shape functions approach this limiting result even for moderate values of  $\sigma$ . Also shown is the drag corresponding to these cases.

$$\frac{D}{q_0 l^2 (\Delta S^*_{max})^2} = \frac{3}{4B(\sigma)[T(\sigma)]^2} \quad (76)$$

which shows a similar drop from the  $\sigma=0$  value as  $\sigma$  is increased. Again, the effective fineness ratio of the bodies is increasing with  $\sigma$ , and, if frontal area exposed to the stream is held fixed, the maximum thickness of the excrescence vanishes as  $1/\sigma$  for large  $\sigma$ . The departure of the geometric variation from the slender-body case is most pronounced near the nose,  $\eta=0$ , where the slope is given by

$$\frac{dS^*(\eta)}{d\eta} = \frac{3\pi}{8} \frac{V_e^*}{B(\sigma)} (1+4\sigma) \sqrt{\frac{2\sigma}{1+2\sigma}} \quad (77)$$

which vanishes only as  $\sqrt{\sigma}$  for  $\sigma \rightarrow 0$ .

**The optimum body of given caliber.**—In this case, the maximum cross-section occurs at  $\eta=1$  so there is no longitudinal symmetry. Figure 12 shows, for several values of the parameter  $\sigma$ , the optimum, equal-caliber, incremental cross-section area given by equation (71). The inset shows the drag as a function of  $\sigma$ ; from equation (74)

$$\frac{D}{q_0 \left( \frac{\Delta S^*}{l} \right)^2} = \frac{4}{\pi(1+4\sigma)}$$

Again in this case, the closeness of the optimum distributions as  $\sigma$  increases to the two-dimensional value ( $\sigma \rightarrow \infty$ ) is noticeable. This point has also been made by Ferrari in reference 5 where problems similar to ours are treated by a different approach. If the expression for cross-section area (eq. (71)) is expanded in powers of  $1/\sigma$ , it is found that

$$\frac{\Delta S^*(\eta, \sigma)}{\Delta S^*(1, \sigma)} = \eta - \frac{\eta(1-\eta)(1-2\eta)}{32} \left( \frac{1}{\sigma} \right)^2 + \dots \quad (78)$$

which shows the smallness of the correction to the two-dimensional result for moderate values of  $\sigma$ .

**RECIPROCITY RELATIONS**

**The optimum body of given volume.**—The longitudinal and radial perturbation velocities can be determined by substituting the derivative of the source-distribution function (eq. (57)) into the formulae (29) and (30). We find, at any point  $(x, r)$  ( $r \geq R$ ) in the field

$$\frac{\varphi_x(x, r)}{U_0} = \frac{\mu_1}{8\pi q_0} \frac{1}{\sqrt{[x+\beta(r+R)][l-x+\beta(r+R)]}} \{ 4[x+\beta(r+R)][l-x+\beta(r+R)] E + [l(l+4\beta R) - 4(l+2\beta R)(l-x+\beta r+\beta R)] K + 4(l+2\beta R)(l-2x)\Pi(\alpha^2, k) \} \quad (79a)$$

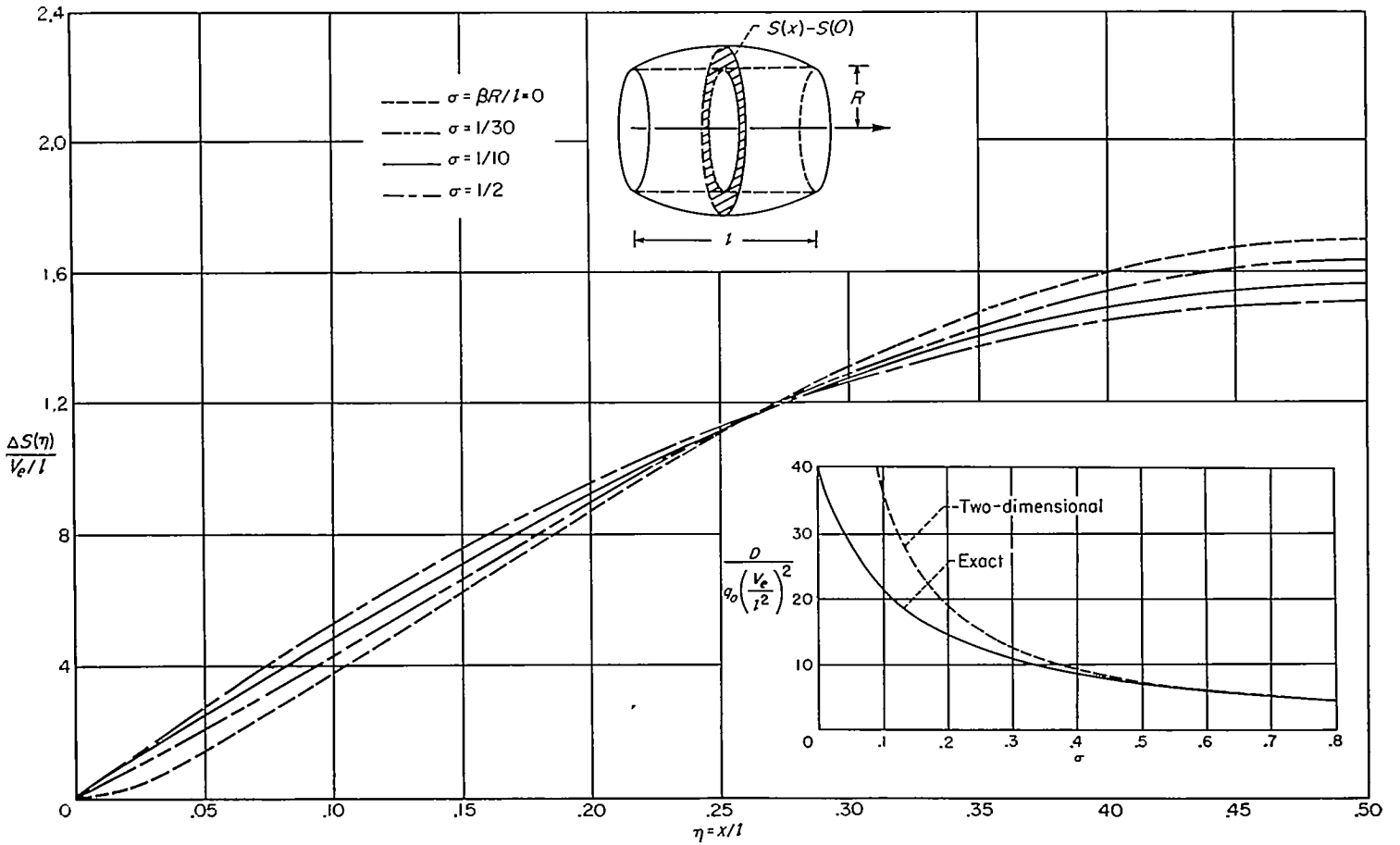


FIGURE 10.—Geometry and drag characteristics of optimum bodies of equal volume.

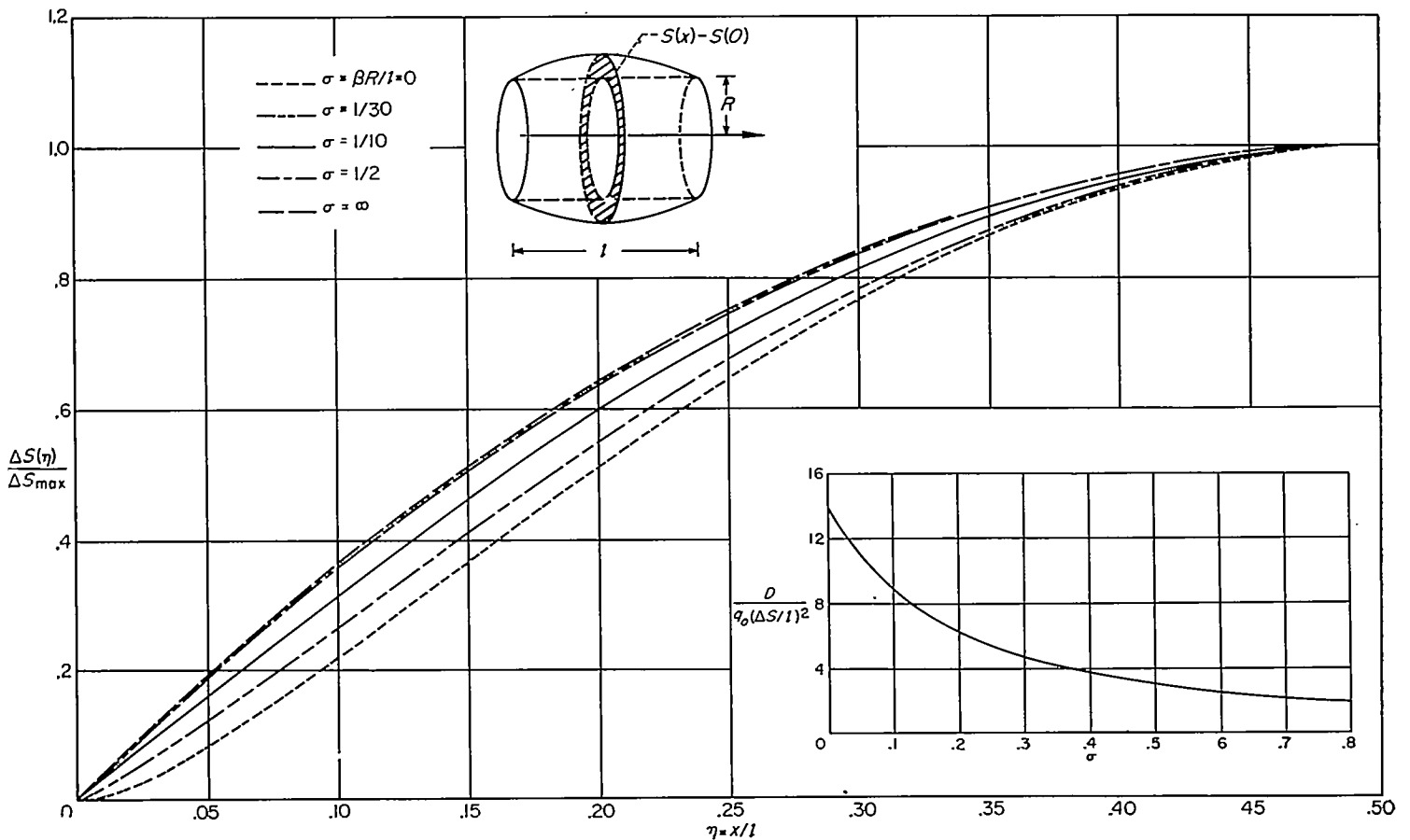


FIGURE 11.—Geometry and drag characteristics of optimum bodies of given volume (bodies having equal additional frontal area).

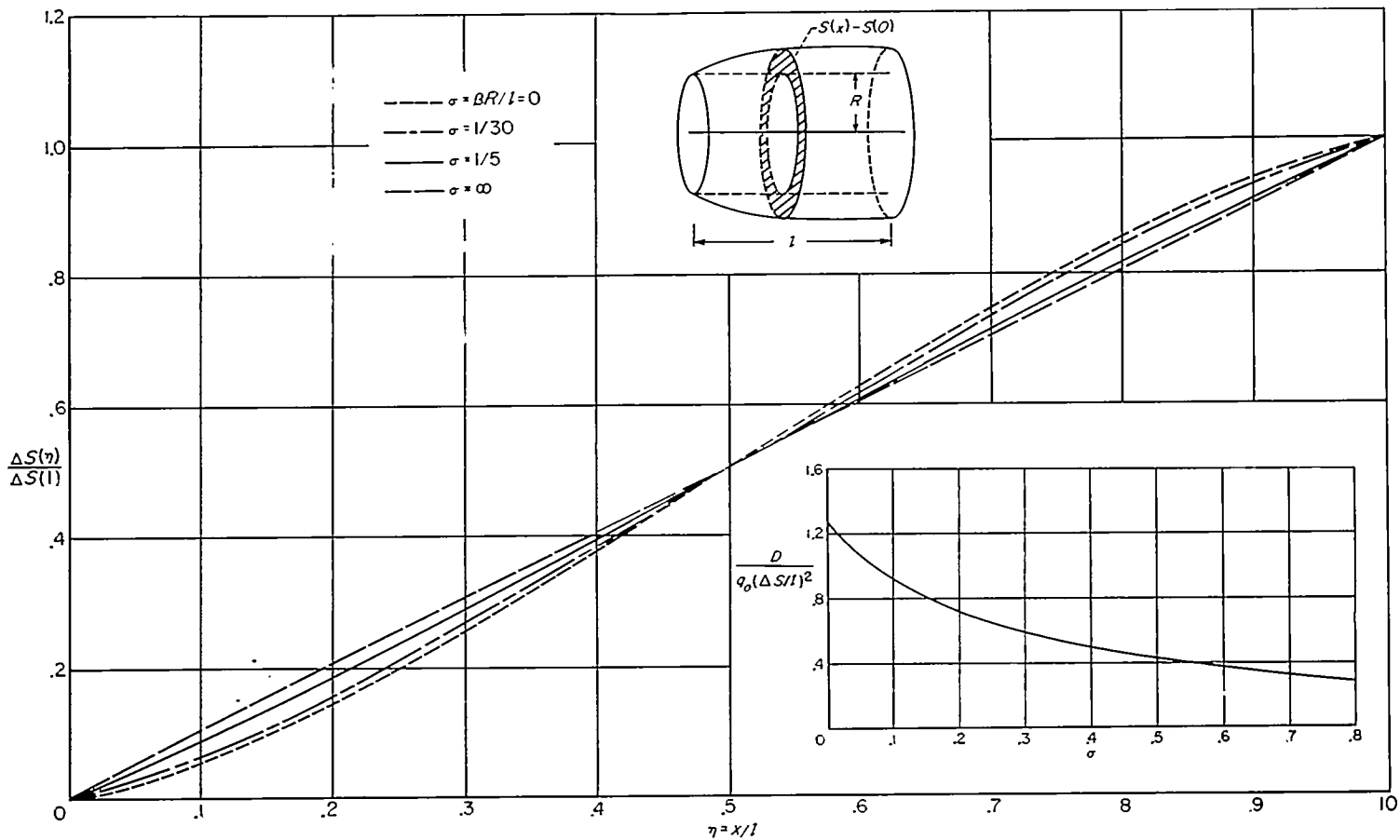


FIGURE 12.—Geometry and drag characteristics of optimum bodies of given caliber.

$$\frac{\varphi_r(x,r)}{U_0} = \frac{\mu_1}{8\pi q_0 r} \frac{1}{\sqrt{[x+\beta(r+R)][l-x+\beta(r+R)]}} \{ (l-2x)[x+\beta(r+R)][l-x+\beta(r+R)]E - \beta r l [l-2x+2\beta(r-R)]K - 4\beta^2 R(r-R)[l-x+\beta(r+R)]K + 4\beta^2(r^2-R^2)(l+2\beta R)\Pi(\alpha^2, k) \} \quad (79b)$$

where now

$$k^2 = \frac{x(l-x)}{[x+\beta(r+R)][l-x+\beta(r+R)]}$$

$$\alpha^2 = \frac{x-\beta(r-R)}{l-x+\beta(r+R)}$$

For the present axis system, the act of reversing the flow amounts to substituting  $l-x$  for  $x$ , and, for the case of the symmetric body, the longitudinal perturbation velocity in the reversed flow is

$$\tilde{u}(x,r) = -u(l-x,r) = -\varphi_x(l-x,r)$$

Now, from equation (40), pressure in the combined field is given by

$$P = -\rho_0 U_0 (u + \tilde{u}) = -\rho_0 U_0 [\varphi_x(x,r) - \varphi_x(l-x,r)] \quad (80)$$

In order to verify this relation using equation (79a), the following result, which can be derived from formulae of reference 20, section 400, will be useful: Let

$$V_1(x) = \Pi(\alpha^2, k)$$

then

$$V_1(x) + V_1(l-x) = K + \frac{\pi}{2} \frac{\sqrt{[l-x+\beta(r+R)][x+\beta(r+R)]}}{l+2\beta R}$$

This, together with the fact that the modulus  $k$  is invariant to the substitution of  $l-x$  for  $x$ , enables us to write immediately

$$P = \frac{\mu_1}{2} (l-2x) \quad (81)$$

Differentiating equation (81) we find

$$P' + \mu_1 = 0 \quad (82)$$

which agrees with the criterion for minimum drag with given volume established in equation (47). The Lagrange multiplier  $\mu_1$  is therefore identified as the pressure gradient in the combined flow field. It will be noted that equations (81) and (82) hold everywhere within the enveloping forward and rearward Mach cones of the quasi-cylindrical body (see fig. 4).

Now considering the radial component of perturbation velocity  $\varphi_r$ , we find, using the relations mentioned just previously

$$\frac{\varphi_r(x,r)}{U_0} + \frac{\varphi_r(l-x,r)}{U_0} = \frac{\beta^2(r^2-R^2)}{4q_0 r} \mu_1 \quad (83)$$

so that the relation

$$\varphi_r(x,r) = -\varphi_r(l-x,r)$$

is satisfied on the quasi-cylinder itself, that is, when we set  $r=R$ .

The optimum body of given caliber.—For this case we find the following equations for the perturbation velocities:

$$\frac{\varphi_x(x,r)}{U_o} = -\frac{\lambda(l+2\beta R)}{2\pi q_o \sqrt{[x+\beta(r+R)][l-x+\beta(r+R)]}} [K-2\Pi(\alpha^2, k)] \quad (84a)$$

$$\frac{\varphi_r(x,r)}{U_o} = -\frac{\lambda}{2\pi q_o r \sqrt{[x+\beta(r+R)][l-x+\beta(r+R)]}} \{ [x+\beta(r+R)][l-x+\beta(r+R)]E - \beta r(l+2\beta R)K \} \quad (84b)$$

where the elliptic integrals have the same modulus and parameter as in the previous section.

In this case, the pressure in the combined flow field is

$$P = -\rho_o U_o [\varphi_x(x,r) + \varphi_x(l-x,r)] \quad (85)$$

which gives

$$P = -\lambda \quad (86)$$

so that in this instance, pressure itself is constant in the combined flow field.

From equation (84b), we see that

$$\varphi_r(x,r) = \varphi_r(l-x,r) \quad (87)$$

since the modulus of the elliptic integrals is invariant to the change  $x \rightarrow l-x$ .

Uses of reciprocity relations.—The reciprocity relations serve the dual function of checking the derived perturbation potential against minimization criteria based on other considerations (see eq. (47)) and of relating the Lagrangian multipliers to the pressure or pressure gradient in the combined flow field. Equations (81) and (86) also reveal that the expressions for pressure in the combined flow field hold, independently of  $r$ , throughout the entire region within the enveloping cones of the bodies. These results are generalizations of a similar effect noted in reference 19, where the combined pressure field associated with a Sears-Haack body was shown to have a constant gradient within the enveloping cones. In the latter reference, this property of the minimum-drag body was used to expedite the calculation of interference drag with a satellite body lying within the enveloping cones. Similar methods could obviously be applied to the present configurations.

AMES AERONAUTICAL LABORATORY  
 NATIONAL ADVISORY COMMITTEE FOR AERONAUTICS  
 MOFFETT FIELD, CALIF., Nov. 22, 1954

## APPENDIX A

### SUMMARY OF FORMULAE FOR THE OPTIMUM BODIES

The formulae derived in the text for the body shape function, pressure coefficient, and drag of optimum bodies having given volume or given caliber are repeated here for convenience. The type of configuration treated, and the nomenclature, are shown in figure 13.

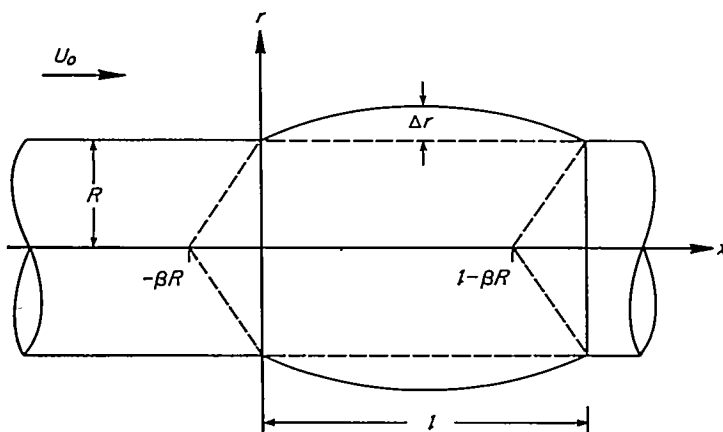


FIGURE 13.—Body and associated nomenclature used in drag minimization.

#### THE OPTIMUM BODY OF GIVEN VOLUME

The variation of  $\Delta S$  for the optimum body with given volume is

$$\Delta S(x) = -\frac{V_o}{l^4 B\left(\frac{\beta R}{l}\right)} \sqrt{(x+2\beta R)(l-x+2\beta R)} \{ x(l-x)E(k) - \beta R(l-4\beta R)[K(k) - E(k)] \} \quad (A1)$$

where

$$\Delta S(x) = \pi[(R + \Delta r)^2 - R^2]$$

$V_o$  = volume of exposed portion

$B\left(\frac{\beta R}{l}\right) = B(\sigma)$  function defined in equation (60a) and shown in figure 7

$K(k)$  = complete elliptic integral of first kind of modulus  $k$

$E(k)$  = complete elliptic integral of second kind of modulus  $k$

$$k^2 = \frac{x(l-x)}{(x+2\beta R)(l-x+2\beta R)}$$

Examples of optimum bodies for a few values of the parameter  $\beta R/l$  are shown in figures 10 and 11.

The pressure coefficient on the body is

$$C_p = \frac{p-p_o}{q_o} = -2 \frac{u}{U_o} = \frac{3}{2\pi} \frac{V_o}{l^4 B\left(\frac{\beta R}{l}\right)} \times \frac{4(x+2\beta R)(l-x+2\beta R)E - [l(l+4\beta R) - 4(l+2\beta R)(l-x+2\beta R)]K + 4(l+2\beta R)(l-2x)\Pi(\alpha^2, k)}{\sqrt{(x+2\beta R)(l-x+2\beta R)}} \quad (A2)$$

where  $\Pi(\alpha^2, k)$  is a complete elliptic integral of third kind of modulus  $k$  and parameter  $\alpha^2$  (in the notation of ref. 20). The parameter  $\alpha^2$  is given by

$$\alpha^2 = \frac{x}{l-x+2\beta R}$$

Figure 14 shows some plots of  $C_p/(V_e/l^3)$  versus  $x/l$  for a few values of the parameter  $\beta R/l$ .

The wave drag of this optimum body is given by

$$\frac{D}{q_0} = 3 \frac{V_e^2}{l^4 B \left(\frac{\beta R}{l}\right)} \quad (A3)$$

The variation of drag with  $\beta R/l$  is shown in figures 10 and 11.

THE OPTIMUM BODY OF GIVEN CALIBER

The variation of  $\Delta S(x)$  for the optimum body of given caliber is

$$\Delta S(x) = \frac{2}{\pi} \frac{\Delta S(l)}{l(l+4\beta R)} \times \frac{l(l+2\beta R)(l+4\beta R)\Pi(\alpha^2, k) - (l-2x)(x+2\beta R)(l-x+2\beta R)E - l(l+2\beta R)(l-x+2\beta R)K}{\sqrt{(x+2\beta R)(l-x+2\beta R)}} \quad (A4)$$

where the symbols have been defined above. Examples of optimum bodies for a few values of the parameter  $\beta R/l$  are shown in figure 12.

The pressure coefficient on the body is given by

$$C_p = \frac{8}{\pi^2} \frac{\Delta S(l)}{l} \frac{l+2\beta R}{l+4\beta R} \frac{2\Pi(\alpha^2, k) - K}{\sqrt{(x+2\beta R)(l-x+2\beta R)}} \quad (A5)$$

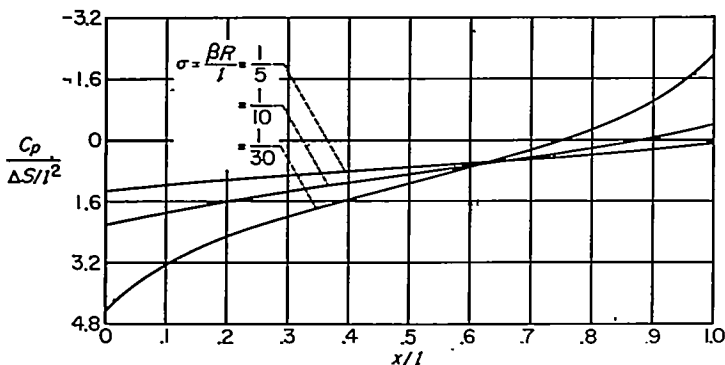


FIGURE 15.—Pressure distributions for various cases of the optimum body of given caliber.

Figure 15 shows some plots of  $\frac{C_p}{\Delta S(l)/l^2}$  versus  $x/l$  for several values of the parameter  $\beta R/l$ .

The drag of this body is

$$\frac{D}{q_0} = \frac{4}{\pi(l+4\beta R)} \frac{[\Delta S(l)]^2}{l} \quad (A6)$$

and its variation with  $\beta R/l$  is shown in figure 12.

REFERENCES

1. Ward, G. N.: The Approximate External and Internal Flow Past a Quasi-Cylindrical Tube Moving at Supersonic Speeds. *Quart. Jour. Mech. and Appl. Math.*, vol. I, pt. 2, June 1948, pp. 225-245.
2. Lighthill, M. J.: *Supersonic Flow Past Bodies of Revolution*. R. & M. No. 2003 British A. R. C., 1945.
3. Parker, Hermon M.: Minimum Drag Ducted and Pointed Bodies of Revolution Based on Linearized Supersonic Theory. NACA Rep. 1213, 1955. (Formerly NACA TN 3189)
4. Ferrari, Carlo: Determination of the External Contour of a Body of Revolution with a Central Duct so as to Give Minimum Drag in Supersonic Flow, With Various Perimetral Conditions

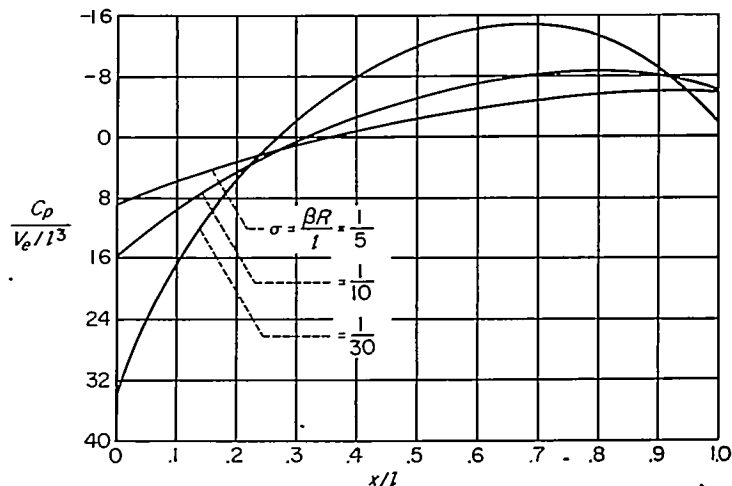


FIGURE 14.—Pressure distributions for various cases of the optimum body of given volume.

Imposed Upon the Missile Geometry. Cornell Aero. Lab. Rep. AF-814-A-1, Mar. 1953.

5. Ferrari, Carlo: Determination of the External Contour of a Body of Revolution With a Central Duct so as to Give Minimum Drag in Supersonic Flow, With Various Perimetral Conditions Imposed Upon the Missile Geometry. Part III. Numerical Application. Cornell Aero. Lab. Rep. AF-8H-A-2, Nov. 1953.
6. Churchill, Ruel V.: *Modern Operational Mathematics in Engineering*. McGraw-Hill Book Co., Inc., N. Y., 1944.
7. Heaslet, Max. A., and Lomax, Harvard: Further Remarks Concerning Integral Transforms of the Wave Equation. *Jour. Aero. Sci.*, vol. 21, no. 2, Feb. 1954, p. 142.
8. Watson, G. N.: *A Treatise on the Theory of Bessel Functions*. Second ed. Cambridge Univ. Press, 1952.
9. Staff of Bateman Manuscript Project: *Tables of Integral Transforms*. Vol. I. McGraw-Hill Book Co., 1954.
10. Lamb, Horace: *Hydrodynamics*. Sixth ed., Dover Pub., 1945.
11. Ward, G. N.: Supersonic Flow Past Slender Pointed Bodies. *Quart. Jour. Mech. and Appl. Math.*, vol. II, pt. 1, 1949, pp. 75-97.
12. Mersman, W. A.: Numerical Calculation of Certain Inverse Laplace Transforms. Vol. 2 of Proc. Intl. Cong. of Mathematicians, Amsterdam, 1954.
13. Jones, Robert T.: The Minimum Drag of Thin Wings in Frictionless Flow. *Jour. Aero. Sci.*, vol. 18, no. 2, Feb. 1951, pp. 75-81.
14. Heaslet, Max. A., and Spreiter, John R.: Reciprocity Relations in Aerodynamics. NACA Rep. 1119, 1953. (Formerly NACA TN 2700)
15. Heaslet, Max. A., and Lomax, Harvard: Supersonic and Transonic Small Perturbation Theory. (Sec. D. of General Theory of High Speed Aerodynamics. Vol. VI of High Speed Aerodynamics and Jet Propulsion, W. R. Sears, ed., Princeton Univ. Press, 1954.)
16. Sears, William R.: On Projectiles of Minimum Wave Drag. *Quart. App. Math.*, vol. IV, no. 4, Jan. 1947, pp. 361-366.
17. Haack, W.: Geschossformen kleinsten Wellen-widerstandes. Lilienthal-Gesellschaft für Luftfahrtforschung, Bericht 130, Teil 1, October 9-10, 1941, pp. 14-28.
18. von Kármán, Th.: The Problem of Resistance in Compressible Fluids. Proc. of the 5th Volta Congress (1935), Rome. Sept. 30-Oct. 6, 1935. (Also published as C. I. T., Guggenheim Aero. Lab. Pub. 75.)
19. Friedman, Morris D., and Cohen, Doris: Arrangement of Fusiform Bodies to Reduce the Wave Drag. NACA TN 3345, 1954 (Formerly NACA RM A51I20)
20. Byrd, Paul F., and Friedman, Morris D.: *Handbook of Elliptic Integrals for Engineers and Physicists*. Springer-Verlag (Berlin), 1954.